Journal of Geophysical Research: Atmospheres

RESEARCH ARTICLE
10.1029/2018JD029231

Source Sector Attribution of CO_2 Emissions Using an Urban CO/CO_2 Bayesian Inversion System

B. J. Nathan[1], T. Lauvaux[1], J. C. Turnbull[2,3], S. J. Richardson[1], N. L. Miles[1], and K. R. Gurney[4]

[1]Department of Meteorology and Atmospheric Science, The Pennsylvania State University, State College, PA, USA, [2]GNS Science, Wellington, New Zealand, [3]CIRES, University of Colorado Boulder, Boulder, CO, USA, [4]Arizona State University, Phoenix, AZ, USA

Key Points:
- Sector-based inversion of emissions was demonstrated by jointly assimilating CO and CO_2 mole fractions over Indianapolis
- Top-down multispecies measurements and high-resolution bottom-up sectoral emissions are in relative agreement over Indianapolis
- Current uncertainties in sectoral emissions of non-CO_2 trace gases limit our ability to quantify sectoral CO_2 emissions

Correspondence to:
B. J. Nathan,
brian.nathan@mio.osupytheas.fr

Citation:
Nathan, B. J., Lauvaux, T., Turnbull, J. C., Richardson, S. J., Miles, N. L., & Gurney, K. R. (2018). Source sector attribution of CO_2 emissions using an urban CO/CO_2 Bayesian inversion system. *Journal of Geophysical Research: Atmospheres*, *123*, 13,611–13,621. https://doi.org/10.1029/2018JD029231

Received 29 JUN 2018
Accepted 13 NOV 2018
Accepted article online 20 NOV 2018
Published online 13 DEC 2018

Author Contributions
Conceptualization: B. J. Nathan, T. Lauvaux
Data curation: J. C. Turnbull, S. J. Richardson, N. L. Miles, K. R. Gurney
Funding Acquisition: T. Lauvaux, J. C. Turnbull
Methodology: B. J. Nathan, T. Lauvaux
Validation: B. J. Nathan, T. Lauvaux, J. C. Turnbull, S. J. Richardson, N. L. Miles, K. R. Gurney
Writing - Original Draft: B. J. Nathan, T. Lauvaux
Formal Analysis: B. J. Nathan, T. Lauvaux
Investigation: B. J. Nathan, T. Lauvaux, J. C. Turnbull
Resources: T. Lauvaux, J. C. Turnbull
Supervision: T. Lauvaux
Visualization: B. J. Nathan, T. Lauvaux
Writing - review & editing: B. J. Nathan, T. Lauvaux, J. C. Turnbull, S. J. Richardson, N. L. Miles, K. R. Gurney

Abstract We assimilate multiple trace gas species within a single high-resolution Bayesian inversion system to optimize CO_2ff emissions for individual source sectors. Starting with carbon monoxide (CO), an atmospheric trace gas with fairly well-known emissions, we use emission factors of CO and CO_2ff (called R_{CO}) defined for each source sector to enable us to jointly use CO and CO_2 atmospheric mole fractions to constrain CO_2ff sectoral emissions. We first show that our combined CO-CO_2 inversion is theoretically capable of estimating the relative magnitude of sectoral emissions for two, specially defined sectors over Indianapolis, while CO_2-only inversions failed at quantifying sectoral emissions. When assimilating hourly mole fractions collected over 4 months, inverse sectoral emissions converge toward high-resolution CO_2ff *bottom-up* emissions from Hestia. The emission ratios between the two sectors agree within 15% with Hestia across various inversion configurations. The assimilation of CO mole fractions preferentially improves flux estimates from traffic emissions, because the CO levels originating from the combustion engine sector are large relative to those from other economic sectors. In a further investigation, we find that including an additional third tracer sensitive to the other sectors only slightly improves the accuracy of the inversion compared to our current two-sector inversions with CO and CO_2 mole fractions. We finally examined the impact of errors in trace gas emission factors and quantify their relative impact on sector-based inverse emissions. We conclude that multispecies inversions can constrain sectoral emissions at policy-level uncertainties if trace gas emission factors are sufficiently well known at the city level.

Plain Language Summary As global urbanization grows rapidly, policymakers need to collect information about the relative changes in anthropogenic emissions from the different sectors of the economy in order to make informed policy decisions. However, bottom-up approaches, relying on activity data, remain the only methods able to produce emissions at the sector level. In our study, we investigate whether atmospheric inversions can help inform about CO_2 emissions from specific sectors of the economy through the inclusion of atmospheric measurements of non-CO_2 trace gases. Our results demonstrate that the joint optimization of atmospheric trace gases, here CO_2 and carbon monoxide (CO), within a single inversion framework can help characterize sector-level emissions of CO_2 over the city of Indianapolis, IN. Emissions from traffic are constrained in parallel with the other sectors of activities. City mitigation policies targeting specific sectors of the local economy can now be better evaluated by atmospheric measurements, with a nearly independent approach to provide more confidence in the effectiveness of emission reduction measures. These results will have important implications for policy makers and the carbon cycle community, reinforcing the link between policy decisions and future climate projections.

1. Introduction

Anthropogenic CO_2 emissions continue to increase, causing atmospheric concentrations to increase at their fastest observed decadal rate (IPCC, 2014; Le Quéré et al., 2017). A significant portion of these emissions originate from urban areas (about 70%), and this number is expected to increase as forecasts predict an additional 2.5–3 billion people relocating to urban areas by 2050 (Seto et al., 2014). Accurate urban emission quantification and reporting will be paramount to helping policymakers decide on appropriate mitigation strategies (e.g., Ciais et al., 2014). Short of a few scientifically intensive efforts in a handful of cities (e.g., Gurney et al., 2012), current urban emissions quantification is primarily composed of self-reported efforts following one of

a few standardized protocols (Carney & Shackley, 2009; Ewing-Thiel & Manarolla, 2011; Wong et al., 2014; WRI / WBCSD, 2004). The self-reported inventories, in particular, may contain biases/errors when used to diagnose emissions or as a baseline to emissions projection. As noted by Nisbet and Weiss (2010), atmospheric methods could provide additional constraints on anthropogenic carbon emissions to better inform policymakers about their decisions (Hutyra et al., 2014). Recent studies have demonstrated how atmospheric inversions could help assess urban-scale CO_2 emissions over time and space (e.g., Bréon et al., 2015; Lauvaux et al., 2016; Nickless et al., 2018) but policy decisions require information for individual sectors of the economy, and with subcity spatial resolution (Gurney, 2015).

The use of additional atmospheric tracer species has been studied for separating CO_2 atmospheric signals into components, such as fossil fuel CO_2 emissions from biogenic signals at continental scales (e.g., Boschetti et al., 2017) or for whole-city emissions (e.g., Wong et al., 2015). Aside from the use of $^{14}CO_2$ to separate out fossil-fuel-related CO_2 (CO_2ff) from biogenic and other CO_2 sources (e.g., Levin et al., 2003; Turnbull et al., 2015), studies have also looked at $\delta^{13}C$ to further distinguish between the gasoline-related, natural-gas-related, and coal-related influences (e.g., Clark-Thorne & Yapp, 2003; Newman et al., 2016). Some trace gases are also known to have relationships with CO_2ff economic sectors, which could, in theory, be used to help partition a CO_2ff signal. For example, HFC-125 is a halocarbon used mainly for commercial purposes (O'Doherty et al., 2009; Velders et al., 2009). SF_6 is primarily used as a spark-quencher in high-voltage switchgears at electrical transmission and distribution systems (Maiss & Brenninkmeijer, 1998). Acetylene, CO, and most light hydrocarbons are known to be associated primarily with traffic (e.g., Baker et al., 2008; Colvile et al., 2001; Fortin et al., 2005; Warneke et al., 2007; Whitby & Altwicker, 1967). Among all the tracers for CO_2ff emissions, CO is the most widely used, largely due to the relative ease of measurement and the large body of research that informs the sources and sinks of CO in the atmosphere. CO is coemitted with CO_2 from the incomplete burning of fossil fuels, thus is directly related to CO_2ff emissions (e.g., Meijer et al., 1996; Newman et al., 2013; Turnbull et al., 2015). However, in order to assimilate atmospheric trace gases for accurate sector attribution, emission rates of these gases need to be known for each economic sector and for specific geographic locations (Nathan et al., 2018). Indeed, Super et al. (2017) show that CO observations, in particular, can be used to estimate CO_2ff emissions given knowledge of the emission ratios, and that information gleaned from the CO observation footprints (as created using a combination of an Eulerian Model and a Lagrangian Transport model, to get appropriate resolution detail Super et al., 2016) can help to delineate CO_2ff sector contributions.

Atmospheric inversions have traditionally focused on optimizing flux estimates for a single species, like CO_2 (e.g., Bréon et al., 2015; Lauvaux et al., 2016; Rödenbeck et al., 2003) or $^{14}CO_2$ from discrete flask samples (Graven et al., 2018). Recently, attempts have been made to calculate inversions by assimilating both CO_2 and CO data from satellites and airplane measurements (Palmer et al., 2006; Wang et al., 2009). These efforts have found success by focusing on coupling the error correlations to exploit both CO's known relationship to CO_2 and its increased sensitivity to model transport errors. Boschetti et al. (2017) included CH_4 to optimize CO_2 broken down by emission sectors and fuel type. Error-correlation-based multispecies inversions have shown promise in improving CO_2 emission uncertainties on a large scale. However, multispecies inversion based on emission factors across the various CO_2 emission sectors is needed to adequately account for the temporal and spatial variability in non-CO_2 species' emission factors.

In this study, we combine CO and CO_2 mole fractions to improve CO_2ff emission distribution estimates between traffic and nontraffic sectors in the Indianapolis urban environment. This is achieved through a traditional Bayesian inversion calculation modifying the framework from Lauvaux et al. (2016) using prior estimates from the Hestia data product (Gurney et al., 2012) and CO:CO_2ff emission factors (R_{CO}) derived from flask samples (Turnbull et al., 2015; Vimont et al., 2017). Traffic and nontraffic sectors are defined in the inversion to constrain sectoral emissions simultaneously. We then present results after inclusion of real in situ data recorded at five measurement towers in and around Indianapolis during the first 4 months of 2015.

2. Data and Methodology

2.1. The INFLUX Inversion System

The INdianapolis FLUX (INFLUX) project focuses on monitoring greenhouse gas (GHG) emissions from the Indianapolis urban area (Davis et al., 2017; Miles, Richardson, Lauvaux, et al., 2017). Twelve Cavity Ring-Down Spectrometers (Crosson, 2008; Rella et al., 2013) have been deployed to continuously record (1 Hz) GHG (i.e., CO_2, CO, and CH_4) atmospheric mole fractions (Miles, Richardson, Lauvaux, et al., 2017) with calibration

using NOAA tertiary standards (Richardson et al., 2017). Here hourly CO and CO_2 observations from 1 January to 30 April 2015 collected at towers 1, 2, 3, 6, and 9 of the INFLUX network (Miles, Richardson, Davis, et al., 2017) were assimilated in our inversion system. This period of time was chosen both to minimize the biogenic influence (dormant season) and to maximize the amount of available tower data for both trace gas species. Only measurements between 12:00 and 17:00 local standard time were used, when the boundary layer can be assumed to be well mixed. In order to isolate enhancement values from the Indianapolis urban area, the corresponding mole fractions from background sites were subtracted off depending on wind direction as outlined in Lauvaux et al. (2016). WMO data taken at Indianapolis Airport during this 4-month period shows wind mostly coming from the West and South during this period (wind came from between SSW and WNW 38.6% of the time), allowing Tower 1 to serve as the primary logical background tower, with occasional wind from the East (6.6% of the wind came from the ENE, which is the only other cardinal direction with more than 5% contribution during this period), wherein Tower 9 became the logical background tower, again all following the procedure explained in Lauvaux et al. (2016).

With measurements from these towers, we utilize a Bayesian inversion calculation (Tarantola, 2005) to optimize GHG emissions using an analytical formulation, following the equation

$$\mathbf{x} = \mathbf{x_0} + \mathbf{BH}^T(\mathbf{HBH}^T + \mathbf{R})^{-1}(\mathbf{y} - \mathbf{Hx_0}), \tag{1}$$

where $\mathbf{x}$ are the posterior emissions, $\mathbf{x_0}$ are the prior emissions, $\mathbf{y}$ are the observed atmospheric mole fractions, $\mathbf{H}$ are the influence function representing the relationship between surface fluxes and atmospheric mole fractions, $\mathbf{B}$ are the prior error covariance matrix, and $\mathbf{R}$ is the observation error covariance matrix, such that the posterior error matrix is defined as $\mathbf{A}^{-1} = \mathbf{B}^{-1} + \mathbf{H}^T\mathbf{R}^{-1}\mathbf{H}$.

This approach has been previously used to estimate total CO_2 emissions from Indianapolis at 1-km resolution, as described in detail in Lauvaux et al. (2016). We modify the inversion framework by expanding the state vector ($\mathbf{x}$) to include emissions from multiple CO_2ff source sectors. Similarly, we develop the ability to assimilate non-CO_2 observations jointly with CO_2 mole fractions in a consistent framework. Transport errors have previously been calculated and shown to be low (Deng et al., 2017; e.g., error reductions of ~40% in the surface wind direction and ~50% in upper-air wind direction with data assimilation). In our study, error variances are defined using the normalized distance of the χ^2 test, that is, ~2.0 ppm for CO_2 and ~19 ppb for CO, similar to Lauvaux et al. (2016). Error covariances in R (nondiagonal terms) were assumed negligible between the two gases and for each individual gas (i.e., in space and time). While spatial and temporal error correlations might exist, the current literature lacks the required information to prescribe these structures, primarily for transport model errors. An ensemble-based approach at the urban scale would help construct spatial and temporal error covariances in future urban-scale inversion systems.

The prior emissions are provided through the Hestia data product (Gurney et al., 2012), a high-resolution emission product providing estimates by sector, which has been shown to agree within 20% to inversion estimates (Lauvaux et al., 2016), and within 5% when accounting for known biogenic influences (Gurney et al., 2017). Hestia provides CO_2ff emission estimates for Indianapolis for eight source sectors: Airport, Commercial, Industrial, OnRoad, NonRoad, Railroad, Residential, and Electricity Production. For the purposes of this study, these eight sectors are combined into two sectors: *Combustion Engine* (OnRoad + NonRoad) and *Other* (six other sectors). This combination of sectors is performed primarily to balance the source attribution problem into two equally uncertain sectors of activity. Otherwise, the variance ratio will drive the optimal solution toward the least-known sector, since larger errors will become overwhelmingly important in the quadratic form of our minimization problem. The second reason is due to the R_{CO}'s, which are high for sectors using combustion engines but not for the other sectors. We thus partition the problem in two sectors with total CO_2ff flux errors on the same order of magnitude, and two distinct sensitivities to CO emissions, as shown in Figure 1.

The R_{CO}'s for each sector were determined by Turnbull et al. (2015), combining reported CO and CO_2ff emission rates and observations from flask measurements at the same five INFLUX towers (1, 2, 3, 6, and 9). The CO_2ff emission rates for each sector are taken from Hestia. The CO emission rates from the EPA NEI (United States Environmental Protection Agency, 2014) give overall R_{CO} values that are a factor of 2.6 higher than those observed at the INFLUX towers, and the NEI onroad and offroad CO emission rates were reduced to match the observations, described in detail in Turnbull et al. (2015). The R_{CO} for each of the original Hestia sectors in Indianapolis are determined to be as follows (in units of ppb/ppm): 2.0 for Airport, 1.3 for Commercial, 3.1 for

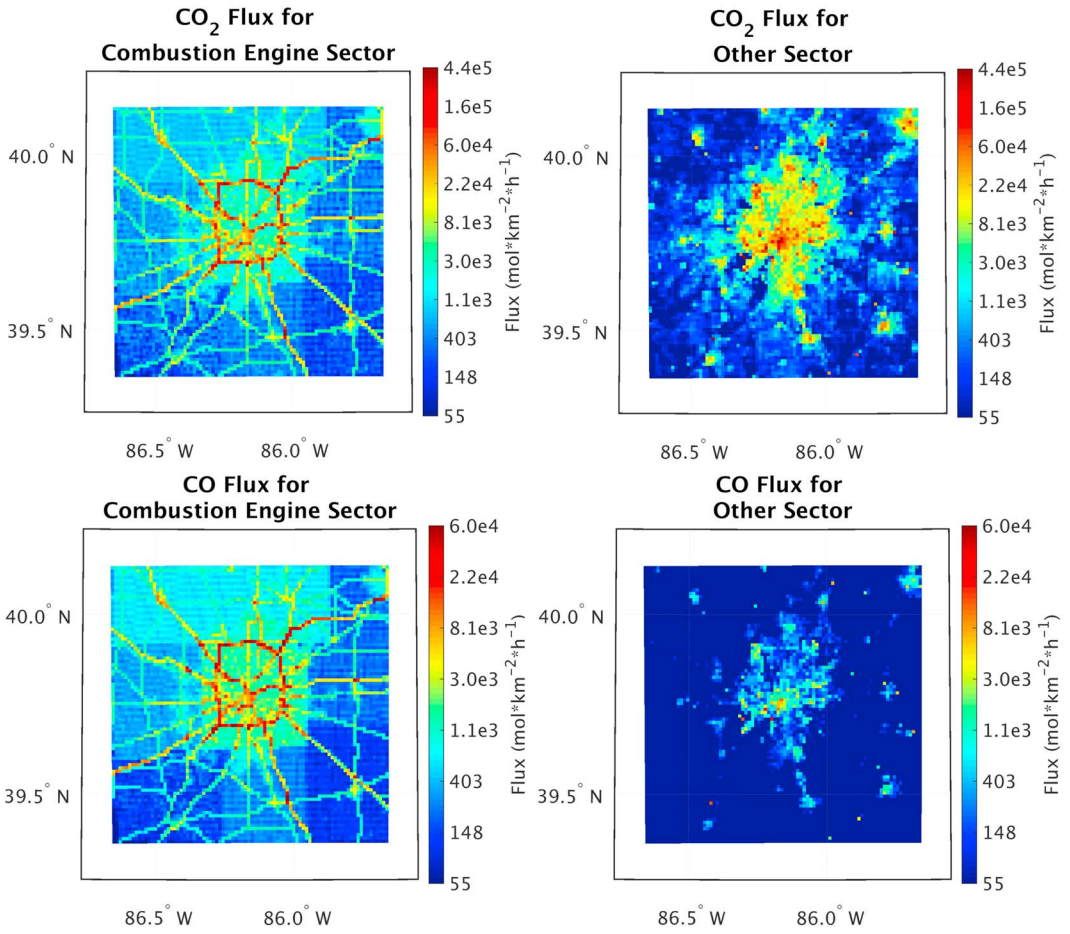

Figure 1. Flux maps for the two source sectors are shown: Combustion Engine and Other. The top row are the CO_2 fluxes and the bottom row are the corresponding emission-factor-derived CO fluxes, on species-relative color scales. The sectors are chosen to have CO_2 fluxes in the same order of magnitude, but where one sector (Combustion Engine) has much higher CO fluxes than the opposing sector (Other).

Industrial, 15 for OnRoad, 45 for NonRoad, 2.0 for Railroad, 0.7 for Residential, and 0.2 for Electricity Production (Turnbull et al., 2015). The emission factors for CO in OnRoad and NonRoad are substantially higher than in any other sector, consistent with measurements of the stable isotopes of CO from INFLUX. During winter in Indianapolis, CO emissions are strongly dominated by traffic sources (Vimont et al., 2017). Thus, creating one sector by combining only onroad and offroad mobile sectors (the Combustion Engine sector) and leaving the remaining sectors in the opposing sector (Other), we also effectively have one *High-CO* sector and one *Low-CO* sector, as shown in Figure 1. The new R_{CO} emission factors for these combined sectors, as scaled by the relative fluxes during the 1 January to 30 April 2015 period of interest, are 17.0 for the Combustion Engine sector and 1.8 for the Other sector. The uncertainties associated with these emission factors, resulting from spatial and temporal variations, can be large. For example, Ammoura et al. (2014) found an uncertainty around 43% for *fluent traffic* in Paris (average vehicle speed above 50 km/hr). Here uncertainties are likely to be smaller, constrained by $^{14}CO_2$ observations. Turnbull et al. (2015) found a flask-based R_{CO} of 8 ± 2 ppb/ppm, with 25% uncertainty. We discuss in section 3.3 the impact of uncertain gas ratios in the sectoral attribution problem.

Prior emission error standard deviations are set to be half of the mean emissions (i.e., 50% uncertainty), excluding strong point sources ($>2.5 \times 10^5$ mol·km^{-2}·hr^{-1}) which are instead set to the median values of the errors across all pixels in the domain. Power plants and industrial emissions are directly reported to the US GHG Reporting Program, hence are assumed to be better constrained compared to other smaller sources (United States Environmental Protection Agency, 2016). Although this assumption may be contested, this error-normalizing procedure also prevents the inversion calculation from disproportionately focusing flux corrections at these large-point-source pixels, allowing for more distributed corrections. In order to

maintain that the whole-city emission error remains equal to 50% of the net emissions, the differences between these extremely large variances and the median values they are reset to are redistributed uniformly over the entire grid (i.e., variances were scaled). Spatial error correlations for both sectors correspond to a combination of sector land cover and an exponentially decaying function similar to Lauvaux et al. (2016), with a 5-km correlation length within each sector. It has been previously shown in Wu et al. (2018) that a spatial error correlation length of between 2 and 8 km is appropriate for CO_2 inversions of Indianapolis to obtain an optimal Degree of Freedom in the Signal—anything larger will cause the city to act as one single unknown when the fluxes are adjusted. At the other extreme, the complete absence of spatial error correlations in B would lack the regularization of the inverse problem, causing a divergence of the solution (Bocquet, 2005). More work needs to be done, especially at the sector level, before any further sensitivity investigation could be fruitful. The prior errors of the Combustion Engine sector are uncorrelated with those of the Other sector, considering that traffic data and vehicle emission factors are unlikely to be affected by the errors in electricity production or the other sectors (e.g., industry, commercial). We optimize a 4-month average for each sector simultaneously, assuming spatial error structures remain unchanged during the winter season. For other seasons, the magnitude of each sector, hence their errors, will vary depending on electricity production levels and house heating, for example. We limit our experiment to one season, avoiding potential biogenic CO sources, and assuming constant error structures for each sector over the 4-month period.

2.2. Inversions with CO_2 and CO

Inversions are first run in the capacity of Observing System Simulation Experiments (OSSEs) to assess the potential of the system. For the period of 1 January to 30 April 2015, measurements are simulated at each available tower for the species-of-interest using influence functions and Hestia emissions with emission-ratio-based flux estimates using the following formula:

$$\text{Enhancement}_j = \sum_{i=1}^{n_j} \left(x_{ji} * H_i\right), \tag{2}$$

where j denotes the source sector of interest (for our study j_{max}=2), x are the Hestia- and emission-ratio-based flux values, H are the influence function values, and the sum across $i \rightarrow n_j$ denotes the cumulative total through the n_j pixels where the influence function overlaps sector j. Note that the CO prior flux maps are derived by multiplying the CO_2ff sectoral flux maps by the appropriate emission factor. For a simultaneous multispecies inversion, the initial state vector $\mathbf{x_0}$ from equation (1) is expanded to include each species' flux maps and $\mathbf{y}$ is expanded to include each species' observations. The influence functions are computed at 1-km resolution using the Weather Research and Forecasting model (Skamarock & Klemp, 2008) coupled with the Lagrangian Particle Dispersion Model (Uliasz, 1994) as described in detail in Lauvaux et al. (2016).

In our pseudo-measurement (cf. equation (2)), we perturb the Hestia fluxes in a repeatable way, creating three different prior flux scenarios (perfect twin experiments). As demonstrated in Lauvaux et al. (2016), Hestia is one of the most advanced emission products, and has been evaluated against atmospheric data. We assume here that Hestia emissions are accurate enough to demonstrate the potential of our inversion, especially for sectoral emissions attribution. By offsetting our initial prior emissions compared to Hestia, we evaluate the ability of the inversion to recover the original sectoral flux ratio. This flux ratio of 1.10 (for $\frac{\text{CombustionEngine}}{\text{Other}}$) is thus altered to create a *high-ratio* prior and a *low-ratio* prior by adding or subtracting a perturbation vector to the Hestia- and emission-factor-based fluxes. The perturbation vector is defined as described above: 50% of the mean flux value at each pixel, except for very-high-emitting sources, as explained in section 2.1. In the high-ratio prior case, we add the Combustion Engine sector's perturbations but only half of the Other sector's perturbations. In the low-ratio case, we subtract off the same respective perturbation amounts. The resulting sector flux ratio numbers are 1.32 and 0.73, respectively. Inversions are then performed using these two prior-ratio cases for three different scenarios: using only CO_2 data, using only CO data, and using both CO_2 and CO data, to be able to compare the relative improvements. After the OSSEs have been performed in this system, real tower data are substituted for the pseudo-measurements and the inversions are recalculated from the same two preset priors.

The upper and lower limits of the error bars around the ratio estimates are calculated using the formula

$$\varepsilon\left(\frac{\text{CE}}{\text{Oth}}\right) = \frac{E(\text{CE}) \pm \sqrt{var(\text{CE})}}{E(\text{Oth}) \pm \sqrt{var(\text{Oth})}}. \tag{3}$$

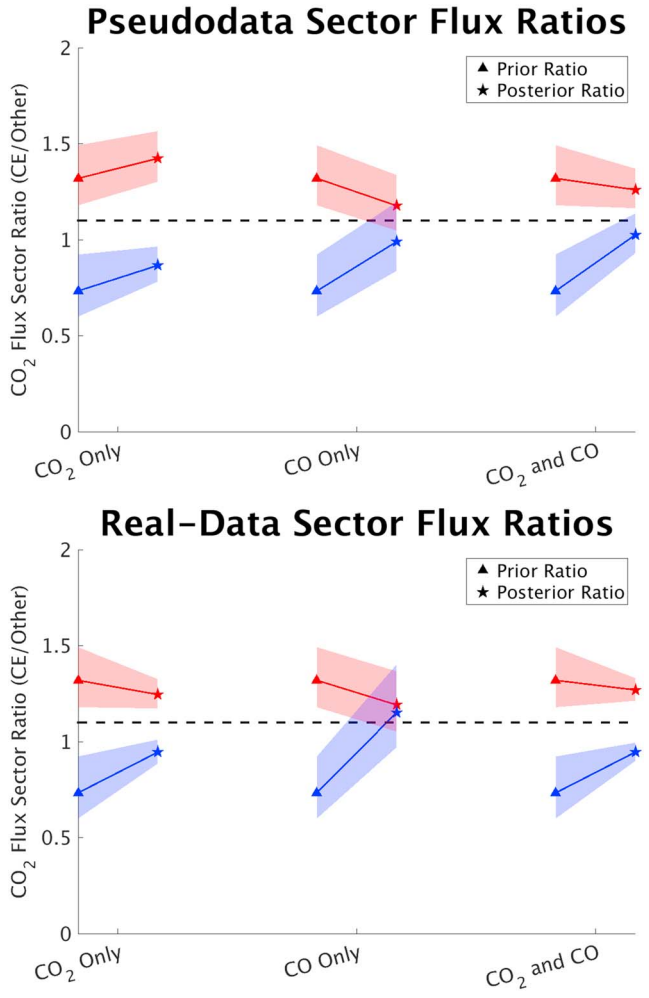

Figure 2. The ratio of fluxes for the Combustion Engine sector against the Other sector is shown both before and after convergence for CO_2 and CO data separately and simultaneously. Two predefined priors are run for each scenario, perturbed from the original flux ratio (shown in the dashed line). The *high-ratio* prior is in red and the *low-ratio* prior is in blue. In the top panel, the CO-only scenario is shown to converge best in the pseudo-data trials. This remains consistent in the bottom panel, though the Hestia dashed line is only an approximation for the *truth* in this case.

Here the upper and lower limit error bars are defined by the range, *E* is the expected value, *var* is the variance, and CE and Oth are the Combustion Engine and Other sector, respectively. In this case, for example, the expectation value of CE when solving for an error bar on a prior flux estimate would be represented by the corresponding prior fluxes for the Combustion Engine sector. The variance of CE would be the sum of the error correlation submatrix for this sector, as extracted from the full multisector error correlation matrix (**B** from equation 1).

2.3. A Hypothetical Other Tracer

We tested the impact of a third atmospheric tracer with a high gas ratio from the Other sector to compensate for CO, which is highly sensitive to the Combustion Engine sector. Here an additional series of pseudo-data inversions are performed. For consistency, the data set and time period are chosen to be INFLUX tower measurements during the period of 1 January to 30 April 2015. The assumptions and constraints of the system are also identical to the previous inversions. Valid measurements for the Other Tracer (OT) are assumed to have been collected only at sites and times when valid CO measurements are available. The flux-scaled mean CO emission factor for Combustion Engine/Other is 17.1, and is defined as such to balance CO. We evaluate the gain in information from this third atmospheric trace gas in our two-sector inversion, reinforcing the observational constraint for sectoral attribution.

The gain after inversion is used to gauge improvement in the posterior estimates where the *true* emissions are known. Compared to analyzing the ratio of sector fluxes (as done in the previous experiments), the gain gives a more direct evaluation of the results, but is unavailable when assimilating real data. The gain is defined as

$$\text{Gain} = 1 - \left(\frac{\sum_{i=1}^{N_j} |x_{\text{true},ji} - x_{\text{post},ji}|}{\sum_{i=1}^{N_j} |x_{\text{true},ji} - x_{\text{prior},ji}|} \right), \quad (4)$$

where *j* denotes the source sector of interest, *x* the Hestia- and emission-ratio-based flux values, for a grid point *i* out of *n* domain pixels. The subscript *true* refers to the true flux, here Hestia scaled by any relevant emission factor, *prior* refers to the prior flux after perturbing the true flux, and *post* refers to the posterior flux estimates after inversion.

3. Results

3.1. Tower Data Inversion

The top panel in Figure 2 shows the results of the pseudo-data inversion with the true (Hestia-based) CO_2ff sectoral ratio (1.10) indicated by the dashed line. The ratio of fluxes for the two sectors (Combustion Engine and Other) were initially perturbed for three inversion scenarios, as described in section 2, while assimilating different atmospheric observations, that is, only CO_2, only CO, and using both CO_2 and CO mole fractions. The inversion scenario that assimilates both CO_2 and CO mole fractions has appreciable convergence back toward the truth (from 1.32 to 1.26 and from 0.73 to 1.02 for the high-ratio and low-ratio priors, respectively), similar to the CO-only scenario (posteriors of 1.18 and 0.99 for the high-ratio and low-ratio priors, respectively), although the CO-only scenario clearly has the best convergence. The CO_2-only scenario fails for the two cases (posteriors of 1.42 and 0.87 for the high-ratio and low-ratio priors, respectively). Since CO_2 is equally sensitive to both sectors, we expect that sectoral fluxes are relatively likely to be adjusted randomly given that they both have comparable uncertainties and no information to disaggregate the mismatches. Therefore, the sector flux ratio is not expected to improve. The CO-only scenario clearly appears to converge back toward the truth. Here the higher sensitivity of CO to the Combustion Engine sector translates into a clear improvement of the sector flux ratio (by improving only the Combustion Engine sector flux), in contrast to the CO_2-only case.

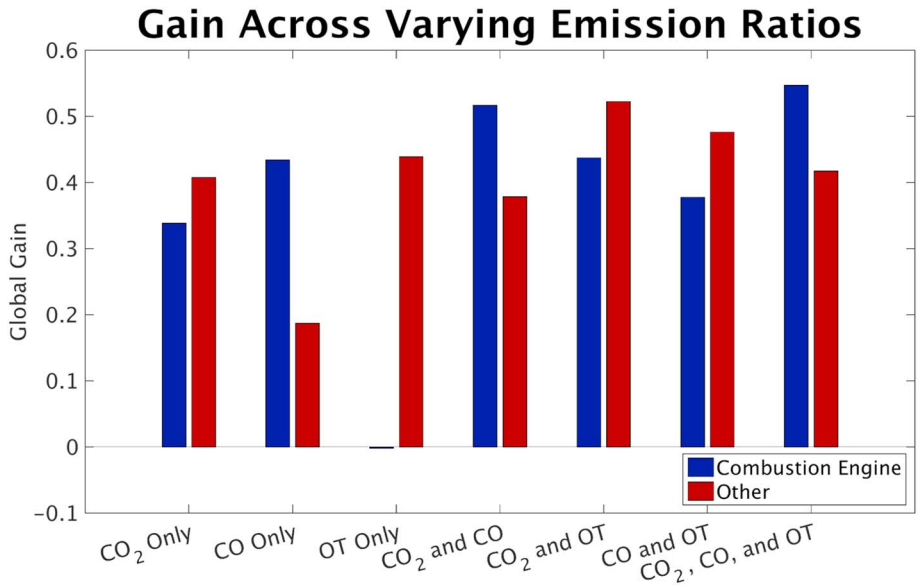

Figure 3. Theoretical gain after inversion for each sector (Combustion Engine and Other) and across inversion scenarios in percent. Gain tends to be greater in a sector with higher average emission factors (e.g., CO-only with Combustion Engine). Data availability and sectoral sensitivity vary by species. OT = Other Tracer.

In Figure 2, the bottom panel shows the results from the same inversion cases and scenarios as in the top panel except with real tower measurement data substituted in place of the pseudo-data. Because of this substitution, the dashed reference line for the Hestia flux ratios (1.10) is unlikely to represent the actual truth, although it is still believed to represent the best first-order approximation and therefore is an acceptable reference for our real-data inversion scenarios. Here the scenario assimilating only CO mole fractions appears to converge the best (from 1.32 to 1.19 and from 0.73 to 1.15 for the high-ratio and low-ratio priors, respectively). This is consistent with the results from the pseudo-data inversions (cf. top panel), which suggested that the CO-only result may be the most trustworthy. The CO_2-only results, on the other hand, are probably the least reliable, despite the apparent trend agreement among both prior-ratio cases (posteriors of 1.35 and 0.94 for the high-ratio and low-ratio priors, respectively). Further, we would expect additional error in the CO_2-based inversions, because, despite having chosen the analysis period to minimize the biogenic influence (following Miles, Richardson, Lauvaux, et al., 2017), there will always be some biogenic CO_2 flux (Gurney et al., 2017; Turnbull et al., 2015). This biogenic flux, which may be between 5% and 20% of the fossil fuel flux in Indianapolis during this period (Turnbull et al., 2015), is not included in the CO_2ff prior flux maps used in the pseudo-data inversion described here, and should hamper the inversion's posterior improvement to some extent. The CO and CO_2 results are, expectedly, somewhere in between the two cases (posteriors of 1.27 and 0.95 for the high-ratio and low-ratio priors, respectively).

3.2. Assimilation of Additional Tracers

To better understand the role of trace gas species and their importance on the sectoral attribution, we present the actual gain for each emission sector in Figure 3, including the hypothetical atmospheric tracer particularly sensitive to the Other sector. All the inversion scenario permutations involving CO_2, CO, and/or OT pseudo-data are shown here. We note that different perturbations would generate higher (resp. lower) gains starting from higher (resp. lower) errors. Hence, the perturbations in the sector flux ratio are kept constant, as we intend to compare the gains of both sectors. The mixed assimilation scenarios combining two to three trace gases show the maximum gain for both sectors (last four bar pairs in Figure 3). The inversion is typically able to improve the prior sectoral emissions by 30% to 50% across all cases. This value will likely reduce in the presence of transport errors and incorrect error definitions in real cases.

The additional trace gas OT has a limited impact in the three-gas simultaneous inversion compared to the other cases mixing two of the three gases. In single-gas cases, the relative gain in one sector over another is shown to be strongly related to gas-ratio sensitivities (e.g., CO-only with the Combustion Engine sector). Similarly, in the inversion with only OT pseudo-data, the gain favors the Other sector. Therefore, in the previous OSSE investigation, the improvement in the relative flux ratio between the sectors resulted mostly from

improving the flux estimates of the most sensitive sector. In particular, we can note that, while the overall gain is consistent with the improvement observed in the sector flux ratio for the CO-only inversions in Figure 2, it is clear that this is driven nearly entirely by improvements in the Combustion Engine sector's fluxes. Additional factors may affect the relative gains from the different inversions, too, with the relative uncertainties between the two sectors being the other most influential. Further factors include the spatial distributions of the sectoral emissions and the number of observations for a given trace gas. For example, CO_2 is measured at more than twice as many INFLUX towers as CO (and, by extension, OT) which drives the gain values and partly mutes the inclusion of a tracer in the inversion.

3.3. Testing Emission Factor Error Impacts

Our reference configuration uses prescribed errors and error structures, all susceptible to impact our results as shown in Lauvaux et al. (2016). Here we consider more specifically the uncertainties associated with emission factors, assumed perfect in our current inversion. R_{CO}'s for traffic emissions — the primary component in our Combustion Engine sector — are known to have high uncertainties and differ significantly study-to-study (e.g., Vimont et al., 2017, and references therein), with some reported uncertainties nearing 50%, for example, Ammoura et al.'s (2014) fluent traffic ratio of $5.68 \pm 2.43 \frac{ppb}{ppm}$. Therefore, we ran pseudo-data trials with CO emission factors that were 15%, 30%, and 50% below observed values and for the same percentages above observed values, only applied to pseudo-data measurements of CO and OT. The other conditions of these inversions were kept constant across all inversions, including prior emissions errors, identical to the *low prior* case.

To determine the impact on the inversion, we assess the change in total gain including both sectors. A reference case with no error in emissions is used to determine the loss in gain following the formula $\frac{new\_gain - ref\_gain}{ref\_gain}$. For the three inversion scenarios without CO_2 measurements (CO-only, OT-only, and CO + OT), the mean gain differences are 0.16 and −0.01 for the ±15% cases, −0.13 and −0.10 for the ±30% cases, and −1.10 and −0.69 for the ±50% cases. We conclude that if the estimated emission rates are within 15% of the observed emission rates, there is nearly no impact on the inversion's results. There is about a 10% deviation in results in the 30% error range, and the inversion becomes unviable near the 50% range. We note that, even in the ±50% uncertainty cases, the gain improvement for the inversion with both non-CO_2 tracers was not substantially different from the inversions with only one non-CO_2 tracer. When CO_2 is included (with no emission rate error) in these same three inversions for the ±50% case, the gain difference values become −0.95 and −0.39, respectively. We conclude here that the inclusion of CO_2 decreases the errors resulting from inaccurate emission ratios just by nature of not having any uncertainty in that dimension. Considering the uncertainties in inventory-based R_{CO} may be large, we conclude here additional observations (e.g., $^{14}CO_2$ and CO) need to be collected, which can substantially reduce the emission factor uncertainty (Levin & Karstens, 2007; Turnbull et al., 2015; Vogel et al., 2010), likely within the desired 15% threshold.

4. Conclusions

In this study, we tested the use of Bayesian inversions to optimize the economic-sector contributions to an urban fossil-fuel CO_2 signal given measurements of tracers of those source sectors. We specifically focus on the Indianapolis urban environment and divide the city into traffic and nontraffic sectors (called the Combustion Engine and Other sectors, respectively), using CO as the traffic-related tracer. Using a high-resolution fossil fuel CO_2 data product and known CO/CO_2ff emission factors, a first-guess prior emission map was constructed for CO in these sectors, allowing for an inversion calculation. Compared to previous studies exploring whole-city emission factors of different trace gases or isotopes (e.g., Newman et al., 2016), we described a formal Bayesian inversion framework to glean information about specific sector contributions to an urban CO_2ff signal inside a metropolitan area. This inversion system provides spatial information, and potentially temporal information if performed over shorter time windows, within the city limits to identify changes in emissions in space and time.

We determined that the relative flux contributions from each sector are able to be improved over Hestia initial estimates through calculating an inversion using either only CO data or a combination of CO and CO_2 data. We also showed that no improvement in this ratio should be expected when running an inversion only using CO_2 data. In theory, it may be possible for CO_2 alone to distinguish the sectors in a scenario where they are spatially distinct and a priori defined based on the transport. But sectors overlap spatially in nearly every urban area. Consequently, the use of a second tracer with a sufficiently large emission factor is deemed to be necessary for this distinction. We found that posterior gains are strongly influenced by the relative uncertainties in the

fluxes and the strength of the emission factors. Assuming uncertainties scale with emission magnitudes, a sector with relatively low fluxes would require an especially sensitive trace gas (i.e., coemitted at a high rate) to ensure substantial posterior improvements. As a result, future studies should identify trace gases emitted primarily by the sectors of interest.

The real-data results agree reasonably well with Hestia sectoral emissions (within 15% across all inversion types), also in agreement with pseudo-data trials, confirming that the Hestia estimate of the sectoral ratio is suitable for first-order evaluation. Given that the system appears to function as intended and that traffic emissions are ~50% of the total CO_2ff emissions for the area, we conclude that current inversion systems could provide relevant traffic sector CO_2 emission information to policymakers. We demonstrated that CO mixing ratios offer an additional constraint on sectoral emissions. Future emission products could combine existing information such as traffic density, flow and velocity, with atmospheric CO observations to provide more reliable estimates of traffic emissions. The framework described here only assimilates atmospheric observations but could be enhanced to assimilate multiple data streams, taking full advantage of the high-resolution information in Hestia and the time coverage of atmospheric data records. Development of urban networks measuring multiple trace gases with high-accuracy can potentially help inform about trends and interannual variability in sectoral emissions.

Additionally, we tested the impact of the availability of an additional tracer for the nontraffic sector. While the inverse sectoral emissions were slightly improved compared to the prior, the inversion results did not significantly improve compared to our original two-gas inversions. In general, our results suggest that flux estimate improvements tend to significantly favor the emission sector for which a species has a higher sensitivity. However, uncertainties in current emission factors can still significantly impair our ability to assimilate multiple species within one single inversion system. While emission factors around 15% away from observed ratios may have negligible impact, ratios near or worse than 50% away can completely negate the benefits of assimilating multiple species. Additional measurements are needed to better quantify the gas ratios between CO_2 and other trace gases before robust inverse sectoral estimates become available.

Acknowledgments
This work has been funded by the National Institute for Standards and Technology (project 70NANB10H245) and the National Oceanic and Atmospheric Administration (grant NA13OAR4310076). The data used in this study can be found at http://datacommons.psu.edu or https://doi.org/10.18113/D37G6P. The authors are grateful for the feedback of the science team of the INFLUX project who helped during the course of this research.

References

Ammoura, L., Xueref-Remy, I., Gros, V., Baudic, A., Bonsang, B., Petit, J. E., et al. (2014). Atmospheric measurements of ratios between CO_2 and co-emitted species from traffic: A tunnel study in the Paris megacity. *Atmospheric Chemistry and Physics*, *14*(23), 12,871–12,882. https://doi.org/10.5194/acp-14-12871-2014

Baker, A. K., Beyersdorf, A. J., Doezema, L. A., Katzenstein, A., Meinardi, S., Simpson, I. J., et al. (2008). Measurements of nonmethane hydrocarbons in 28 United States cities. *Atmospheric Environment*, *42*(1), 170–182. https://doi.org/10.1016/j.atmosenv.2007.09.007

Bocquet, M. (2005). Grid resolution dependence in the reconstruction of an atmospheric tracer source. *Nonlinear Processes in Geophysics*, *12*(2), 219–233. https://doi.org/10.5194/npg-12-219-2005

Boschetti, F., Thouret, V., Maenhout, G. J., Totsche, K. U., Marshall, J., & Gerbig, C. (2017). Multi-species inversion and IAGOS airborne data for a better constraint of continental scale fluxes. *Atmospheric Chemistry and Physics Discussions*, *2017*, 1–37. https://doi.org/10.5194/acp-2017-69

Bréon, F. M., Broquet, G., Puygrenier, V., Chevallier, F., Xueref-Remy, I., Ramonet, M., et al. (2015). An attempt at estimating Paris area CO_2 emissions from atmospheric concentration measurements. *Atmospheric Chemistry and Physics*, *15*(4), 1707–1724. https://doi.org/10.5194/acp-15-1707-2015

Carney, S., & Shackley, S. (2009). The greenhouse gas regional inventory project (GRIP): Designing and employing a regional greenhouse gas measurement tool for stakeholder use. *Energy Policy*, *37*(11), 4293–4302. https://doi.org/10.1016/j.enpol.2009.05.028

Ciais, P., Dolman, A. J., Bombelli, A., Duren, R., Peregon, A., Rayner, P. J., et al. (2014). Current systematic carbon-cycle observations and the need for implementing a policy-relevant carbon observing system. *Biogeosciences*, *11*(13), 3547–3602. https://doi.org/10.5194/bg-11-3547-2014

Clark-Thorne, S. T., & Yapp, C. J. (2003). Stable carbon isotope constraints on mixing and mass balance of CO_2 in an urban atmosphere: Dallas metropolitan area, Texas, USA. *Applied Geochemistry*, *18*(1), 75–95. https://doi.org/10.1016/S0883-2927(02)00054-9

Colvile, R. N., Hutchinson, E. J., Mindell, J. S., & Warren, R. F. (2001). The transport sector as a source of air pollution. *Atmospheric Environment*, *35*(9), 1537–1565. https://doi.org/10.1016/S1352-2310(00)00551-3

Crosson, E. R. (2008). A cavity ring-down analyzer for measuring atmospheric levels of methane, carbon dioxide, and water vapor. *Applied Physics B: Lasers and Optics*, *92*(3 SPECIAL ISSUE), 403–408. https://doi.org/10.1007/s00340-008-3135-y

Davis, K. J., Deng, A., Lauvaux, T., Miles, N. L., Richardson, S. J., Sarmiento, D. P., et al. (2017). The indianapolis flux experiment (INFLUX): A test-bed for developing urban greenhouse gas emission measurements. *Elementa: Science of the Anthropocene*, *5*, 21. https://doi.org/10.1525/elementa.188

Deng, A., Lauvaux, T., Davis, K. J., Gaudet, B. J., Miles, N., Richardson, S. J., et al. (2017). Toward reduced transport errors in a high resolution urban CO_2 inversion system. *Elementa: Science of the Anthropocene*, *5*, 20. https://doi.org/10.1525/elementa.133

Ewing-Thiel, J., & Manarolla, X. (2011). Policy update: ICLEI USA draft framework for measuring and reporting community GHG emissions. *Carbon Management*, *2*(4), 371–375.

Fortin, T. J., Howard, B. J., Parrish, D. D., Goldan, P. D., Kuster, W. C., Atlas, E. L., & Harley, R. A. (2005). Temporal changes in U.S. benzene emissions inferred from atmospheric measurements. *Environmental Science and Technology*, *39*(6), 1403–1408. https://doi.org/10.1021/es049316n

Graven, H., Fischer, M. L., Lueker, T., Jeong, S., Guilderson, T. P., Keeling, R. F., et al. (2018). Assessing fossil fuel CO2 emissions in California using atmospheric observations and models. *Environmental Research Letters*, *13*(6), 13–20. https://doi.org/10.1088/1748-9326/aabd43

Gurney, K. R. (2015). Track urban emissions on a human scale: Cities need to understand and manage their carbon footprint at the level of streets, buildings and communities, urge Kevin Robert Gurney and Colleagues. *Nature*, *525*(7568), 179–181.
Gurney, K. R., Liang, J., Patarasuk, R., O'Keeffe, D., Huang, J., Hutchins, M., et al. (2017). Reconciling the differences between a bottom-up and inverse-estimated FFCO2 emissions estimate in a large US urban area. *Elementa: Science of the Anthropocene*, *5*(44), 1–43. https://doi.org/10.1525/elementa.137
Gurney, K. R., Razlivanov, I., Song, Y., Zhou, Y., Benes, B., & Abdul-Massih, M. (2012). Quantification of fossil fuel CO_2 emissions on the building/street scale for a large U.S. City. *Environmental Science & Technology*, *46*, 12,194–12,202. https://doi.org/10.1021/es3011282
Hutyra, L. R., Duren, R., Gurney, K. R., Grimm, N., Kort, E. A., Larson, E., & Shrestha, G. (2014). Urbanization and the carbon cycle: Current capabilities and research outlook from the natural sciences perspective. *Earth's Future*, *2*, 473–495. https://doi.org/10.1002/2014EF000255
IPCC (2014). Climate change 2014: Synthesis report. Geneva, Switzerland: Intergovernmental Panel on Climate Change. https://doi.org/10.1017/CBO9781107415324
Lauvaux, T., Miles, N. L., Deng, A., Richardson, S. J., Cambaliza, M. O., Davis, K. J., et al. (2016). High resolution atmospheric inversion of urban CO_2 emissions during the dormant season of the indianapolis flux experiment (INFLUX). *Journal of Geophysical Research: Atmospheres*, *121*, 1–24. https://doi.org/10.1002/2015JD024473
Le Quéré, C., Andrew, R. M., Friedlingstein, P., Sitch, S., Pongratz, J., Manning, A. C., et al. (2017). Global carbon budget 2017. *Earth System Science Data Discussions*, *2017*, 1–79. https://doi.org/10.5194/essd-2017-123
Levin, I., & Karstens, U. (2007). Inferring high-resolution fossil fuel CO_2 records at continental sites from combined $^{14}CO_2$ and CO observations. *Tellus, Series B: Chemical and Physical Meteorology*, *59*(2), 245–250. https://doi.org/10.1111/j.1600-0889.2006.00244.x
Levin, I., Kromer, B., Schmidt, M., & Sartorius, H. (2003). A novel approach for independent budgeting of fossil fuel CO_2 over Europe by $^{14}CO_2$ observations. *Geophysical Research Letters*, *30*(23), 2194. https://doi.org/10.1029/2003GL018477
Maiss, M., & Brenninkmeijer, C. A. M. (1998). Atmospheric SF6: Trends sources, and prospects. *Environmental Science & Technology*, *32*(20), 3077–3086. https://doi.org/10.1021/es9802807
Meijer, H., Smid, H., Perez, E., & Keizer, M. (1996). Isotopic characterisation of anthropogenic CO_2 emissions using isotopic and radiocarbon analysis. *Physics and Chemistry of the Earth*, *21*(5-6), 483–487. https://doi.org/10.1016/S0079-1946(97)81146-9
Miles, N., Richardson, S., Davis, K., & Haupt, B. (2017). In-situ tower atmospheric measurements of carbon dioxide, methane and carbon monoxide mole fraction for the Indianapolis Flux (INFLUX) project, Indianapolis, IN, USA. https://datacommons.psu.edu, https://doi.org/10.18113/D37G6P
Miles, N. L., Richardson, S. J., Lauvaux, T., Davis, K. J., Balashov, N. V., Deng, A., et al. (2017). Quantification of urban atmospheric boundary layer greenhouse gas dry mole fraction enhancements: Results from the Indianapolis flux experiment (INFLUX). *Elementa: Science of the Anthropocene*, *5*, 27. https://doi.org/10.1525/elementa.127
Nathan, B., Lauvaux, T., Turnbull, J., & Gurney, K. R. (2018). Investigations into the use of multi-species measurements for source apportionment of the Indianapolis fossil fuel CO_2 signal. *Elementa: Science of the Anthropocene*, *6*(1), 21. https://doi.org/10.1525/elementa.131
Newman, S., Jeong, S., Fischer, M. L., Xu, X., Haman, C. L., Lefer, B., et al. (2013). Diurnal tracking of anthropogenic CO_2 emissions in the Los Angeles basin megacity during spring 2010. *Atmospheric Chemistry and Physics*, *13*(8), 4359–4372. https://doi.org/10.5194/acp-13-4359-2013
Newman, S., Xu, X., Gurney, K. R., Hsu, Y. K., Li, K. F., Jiang, X., et al. (2016). Toward consistency between trends in bottom-up CO_2 emissions and top-down atmospheric measurements in the Los Angeles megacity. *Atmospheric Chemistry and Physics*, *16*(6), 3843–3863. https://doi.org/10.5194/acp-16-3843-2016
Nickless, A., Rayner, P. J., Engelbrecht, F., Brunke, E.-G., Erni, B., & Scholes, R. J. (2018). Estimates of co_2 fluxes over the city of cape town, South Africa, through Bayesian inverse modelling. *Atmospheric Chemistry and Physics*, *18*(7), 4765–4801. https://doi.org/10.5194/acp-18-4765-2018
Nisbet, E., & Weiss, R. (2010). Top-down versus bottom-up. *Science*, *328*(5983), 1241–1243. https://doi.org/10.1126/science.1189936
O'Doherty, S., Cunnold, D. M., Miller, B. R., Mu, J., Mcculloch, A., Simmonds, P. G., et al. (2009). Global and regional emissions of HFC-125 (CHF2CF3) from in situ and air archive atmospheric observations at AGAGE and SOGE observatories. *Journal of Geophysical Research*, *114*, D23304. https://doi.org/10.1029/2009JD012184
Palmer, P. I., Suntharalingam, P., Jones, D. B. A., Jacob, D. J., Streets, D. G., Fu, Q., et al. (2006). Using CO_2:CO correlations to improve inverse analyses of carbon fluxes. *Journal of Geophysical Research*, *111*, 1–11. https://doi.org/10.1029/2005JD006697
Rella, C. W., Chen, H., Andrews, A. E., Filges, A., Gerbig, C., Hatakka, J., et al. (2013). High accuracy measurements of dry mole fractions of carbon dioxide and methane in humid air. *Atmospheric Measurement Techniques*, *6*(3), 837–860. https://doi.org/10.5194/amt-6-837-2013
Richardson, S. J., Miles, N. L., Davis, K. J., Lauvaux, T., Martins, D. K., Turnbull, J. C., et al. (2017). Tower measurement network of in-situ CO_2, CH_4, and CO in support of the Indianapolis FLUX (INFLUX) experiment. *Elementa: Science of the Anthropocene*, *5*, 59. https://doi.org/10.1525/elementa.140
Rödenbeck, C., Houweling, S., Gloor, M., & Heimann, M. (2003). Time-dependent atmospheric CO_2 inversions based on interannually varying tracer transport. *Tellus, Series B: Chemical and Physical Meteorology*, *55*(2), 488–497. https://doi.org/10.1034/j.1600-0889.2003.00033.x
Seto, K. C., Dhakal, S., Bigio, A., Blanco, H., Delgado, G. C., Dewar, D., et al. (2014). Human settlements, infrastructure, and spatial planning. In O. Edenhofer, et al. (Eds.), *Climate change 2014: Mitigation of climate change. Contribution of working group III to the fifth assessment report of the intergovernmental panel on climate change* (pp. 923–1000). Cambridge, UK and New York, NY, USA: Cambridge University Press. https://doi.org/10.1017/CBO9781107415416.018
Skamarock, W. C., & Klemp, J. B. (2008). A time-split nonhydrostatic atmospheric model for weather research and forecasting applications. *Journal of Computational Physics*, *227*(7), 3465–3485. https://doi.org/10.1016/j.jcp.2007.01.037
Super, I., Denier van der Gon, H. A. C., van der Molen, M. K., Sterk, H. A. M., Hensen, A., & Peters, W. (2016). A multi-model approach to monitor emissions of CO2 and CO in an urban-industrial complex. *Atmospheric Chemistry and Physics Discussions*, *17*(September), 1–31. https://doi.org/10.5194/acp-2016-807
Super, I., Denier van der Gon, H. A., Visschedijk, A. J., Moerman, M. M., Chen, H., van der Molen, M. K., & Peters, W. (2017). Interpreting continuous in-situ observations of carbon dioxide and carbon monoxide in the urban port area of Rotterdam. *Atmospheric Pollution Research*, *8*(1), 174–187. https://doi.org/10.1016/j.apr.2016.08.008
Tarantola, A. (2005). Inverse problem theory and methods for model parameter estimation, Siam.
Turnbull, J. C., Sweeney, C., Karion, A., Newberger, T., Lehman, S. J., Tans, P. P., et al. (2015). Toward quantification and source sector identification of fossil fuel CO_2 emissions from an urban area: Results from the INFLUX experiment. *Journal of Geophysical Research: Atmospheres*, *120*, 292–312. https://doi.org/10.1002/2014JD022555
Uliasz, M. (1994). *Lagrangian particle dispersion modeling in mesoscale applications. SMR* (Vol. 706, pp. 23 pp.). Southampton, UK: Computational Mechanics Publications
United States Environmental Protection Agency (2014). 2014 National Emissions Inventory (NEI) data.

United States Environmental Protection Agency (2016). GHG reporting program data sets.
Velders, G. J. M., Fahey, D. W., Daniel, J. S., Mcfarland, M., & Andersen, S. O. (2009). The large contribution of projected HFC emissions to future climate forcing. *Proceedings of the National Academy of Sciences*, *106*(27), 10,949–10,954.
Vimont, I. J., Turnbull, J. C., Petrenko, V. V., Place, P. F., Karion, A., Miles, N. L., & White, J. W. C. (2017). Carbon monoxide isotopic measurements in indianapolis constrain urban source isotopic signatures and support mobile fossil fuel emissions as the dominant wintertime CO source. *Elementa: Science of the Anthropocene*, *5*, 63. https://doi.org/10.1525/elementa.136
Vogel, F. R., Hammer, S., Steinhof, A., Kromer, B., & Levin, I. (2010). Implication of weekly and diurnal 14C calibration on hourly estimates of co-based fossil fuel co_2 at a moderately polluted site in southwestern Germany. *Tellus, Series B: Chemical and Physical Meteorology*, *62*(5), 512–520. https://doi.org/10.1111/j.1600-0889.2010.00477.x
WRI / WBCSD (2004). The GHG protocol for project accounting. Washington, DC: World Resources Institute.
Wang, H., Jacob, D. J., Kopacz, M., Jones, D. B. A., Suntharalingam, P., Fisher, J. A., et al. (2009). Error correlation between CO_2 and CO as constraint for CO_2 flux inversions using satellite data. *Atmospheric Chemistry and Physics*, *9*(19), 7313–7323. https://doi.org/10.5194/acp-9-7313-2009
Warneke, C., McKeen, S. A., de Gouw, J. A., Goldan, P. D., Kuster, W. C., Holloway, J. S., et al. (2007). Determination of urban volatile organic compound emission ratios and comparison with an emissions database. *Journal of Geophysical Research*, *112*, D10S47. https://doi.org/10.1029/2006JD007930
Whitby, R., & Altwicker, E. (1967). Acetylene In the atmosphere: Sources, representative ambient concentrations and ratios to other hydrocarbons. *Atmospheric Environment*, *12*, 1289–1296. https://doi.org/10.1016/0004-6981(78)90067-7
Wong, K. W., Fu, D., Pongetti, T. J., Newman, S., Kort, E. A., Duren, R., et al. (2015). Mapping CH_4:CO_2 ratios in Los Angeles with CLARS-FTS from Mount Wilson, California. *Atmospheric Chemistry and Physics*, *15*(1), 241–252. https://doi.org/10.5194/acp-15-241-2015
Wong, W. K., Sotos, M., Doust, M., Schultz, S., Marques, A., & Deng-Beck, C. (2014). Global protocol for community-scale greenhouse gas emission inventories: An accounting and reporting standard for cities: World Resources Institute. Retrieved from https://ghgprotocol.org/sites/default/files/standards/GHGP_GPC_0.pdf
Wu, K., Lauvaux, T., Davis, K. J., Deng, A., Lopez Coto, I., Gurney, K. R., & Patarasuk, R. (2018). Joint inverse estimation of fossil fuel and biogenic CO2 fluxes in an urban environment: An observing system simulation experiment to assess the impact of multiple uncertainties. *Elementa: Science of the Anthropocene*, *6*(1), 17. https://doi.org/10.1525/elementa.138